Mode Multiplication of Cylindrical Vector Beam Using Raytracing Control

Jing Wang(王晶)[1†], Qingji Zeng(曾庆计)[1†], Haisheng Wu(吴海生)[1], Chuangxin Xie(谢创鑫)[1], Huapeng Ye(叶华朋)[2], Ze Dong(董泽)[3], Dianyuan Fan(范滇元)[1*], and Shuqing Chen(陈书青)[1*]

[1]*Institute of Microscale Optoelectronics, Shenzhen University, Shenzhen 518060, China*
[2]*Guangdong Provincial Key Laboratory of Optical Information Materials and Technology, and Institute of Electronic Paper Displays, South China Academy of Advanced Optoelectronics, South China Normal University, Guangzhou 510006, China*
[3]*School of Information and Electronics, Beijing Institute of Technology, Beijing 100081, China*

(Received 17 June 2024; accepted manuscript online 5 August 2024)

Cylindrical vector beams (CVBs) hold significant promise in mode division multiplexing communication owing to their inherent vector mode orthogonality. However, existing studies for facilitating CVB channel processing are confined to mode shift conversions due to their reliance on spin-dependent helical modulations, overlooking the pursuit of mode multiplication conversion. This challenge lies in the multiplicative operation upon inhomogeneous vector mode manipulation, which is expected to advance versatile CVB channel switching and routing. Here, we tackle this gap by introducing a raytracing control strategy that conformally maps the light rays of CVB from the whole annulus distribution to an annular sector counterpart. Incorporated with the multifold conformal annulus-sector mappings and polarization-insensitive phase modulations, this approach facilitates the parallel transformation of input CVB into multiple complementary components, enabling the mode multiplication conversion with protected vector structure. Serving as a demonstration, we experimentally implemented the multiplicative operation of four CVB modes with the multiplier factors of $N = +2$ and $N = -3$, achieving the converted mode purities over 94.24% and 88.37%. Subsequently, 200 Gbit/s quadrature phase shift keying signals were successfully transmitted upon multiplicative switching of four CVB channels, with the bit-error-rate approaching 1×10^{-6}. These results underscore our strategy's efficacy in CVB mode multiplication, which may open promising prospects for its advanced applications.

DOI: 10.1088/0256-307X/41/9/094202

Cylindrical vector beams (CVBs), which possess spatially rotational-symmetric polarizations manifesting orthogonal vector modes, offer promise for augmenting optical communication capacity through mode division multiplexing.[1–5] Although diverse applications in CVB multiplexing communication have seen achievements, facilitating mode (de)multiplexing, cross-connection, and add-drop multiplexing, they are predominantly driven by mode shift conversions.[6–10] A previously inaccessible manipulation of CVB mode multiplication conversion, which allows for multiplicative operation across input-output modes, is expected to reshape versatile channel processing within CVB-based comprehensive communication networks, thereby promoting scalable channel switching and routing at nodes for signal interconnection.[11–13] However, this key procedure remains a challenge owing to the lack of effective multiplication transformation strategies for the inhomogeneous vector modes. Traditional mode transformations typically focus on mode up/down conversions that utilize spin-conjugated and spin-decoupled phase modulation devices to endow helical modulations to the two spin eigenstates of CVBs.[14–18] Then the CVB mode shift operations are performed via spin-dependent orbital interactions and the conservation of vector modes, but the single helical phase product is confined to mode transition with a fixed interval, i.e., addition or subtraction, leading to its inability to implement mode multiplication operation. Additionally, other optical modulation devices including spiral phase plates,[19,20] spatial light modulators,[21,22] and digital micro-mirror devices[23] have intrinsic uniform polarization responses, limiting their utility for manipulating CVBs with inhomogeneous vector wavefronts. Therefore, the exploration of a feasible modulation technique for multiplying CVB modes still faces challenging.

Apart from harnessing the spin-dependent helical modulation for CVB mode conversion, optical geometric transformation could provide alternative insight. Achieved by the raytracing model that connects a pair of spatial coordinate systems, the optical geometric transformation enables unitary conformal mapping of the complex amplitude distributions of input-output mode fields when obeying a proper coordinate conversion relationship between the systems.[24] Taking advantages of flexible coordinate mapping, strong system compactness and high execution efficiency, this approach has garnered substantial interest in mode manipulation both for sorting and conversion.[25–31]

†These authors contributed equally to this work.
*Corresponding authors. Email: shuqingchen@szu.edu.cn; fandy@cae.cn
© 2024 Chinese Physical Society and IOP Publishing Ltd

For instance, transforming the ring-shaped vector wavefronts of CVBs into tilted ones (situated at distinct lateral positions with respect to the modes) by log-polar or spiral mappings, prompts effective sorting of CVBs.[32,33] On the other hand, this conformal transformation unlocks the potential for operating multiplication in the scalar orbital angular momentum modes, completed by mapping the whole annulus onto multiple complementary annular sectors.[29] Despite considerable endeavors of mode manipulation based on optical geometric transformation, the vector mode multiplication of CVBs remains unrealized.

In accordance with principle of raytracing control, we developed a CVB mode multiplication solution that incorporates polarization-insensitive conformal mapping and phase modulation. By dint of the ray traveling model, the light rays from ring-shaped intensity distribution of input CVB are projected onto defined positions, yielding envelope trajectories from the whole annulus to an annular sector. Imparting the multifold conformal annulus-sector mappings into a one-shot phase modulation, it is possible to transform the CVB mode into multiple complementary components with identical angle ranges, enabling the multiplicative operation of mode. The polarization-insensitive configuration ensures that local linear polarization state of each light ray is unchanged, which reshapes the proper vector filed structure upon CVB mode multiplication conversion. In proof-of-concept experiments, we demonstrated the successful multiplication of four CVB modes (-2, -1, $+1$, $+2$) with the multiplier factors of $N = +2$ and $N = -3$, and the converted mode purities are above 94.24% and 88.37%, respectively. Applying them to a four-channel CVB multiplexing communication with simultaneous polarization division multiplexing (PDM), 200 Gbit/s quadrature phase shift keying (QPSK) signals were successfully transmitted along with multiplicative switching of the mode channels, yielding the bit-error-rate (BER) close to 1×10^{-6}.

To explain the underlying mechanism of raytracing control in CVB, an evolution model of ray traveling was introduced to establish the connection between two coordinate phase planes. In this model, we assume that $\Psi_1(x, y)$ represents the first phase plane and $\Psi_2(u, v)$ indicates the second one both in Cartesian coordinates. When the light ray carrying an initial phase of $\exp(ikz)$ normally illuminates the phase plane Ψ_1, the direction of wave vector k will be altered through phase modulation, which can be expressed as

$$kz + \Psi_1(x, y) = k(a_1 x + b_1 y + z). \tag{1}$$

Here a_1 and b_1 are the direction cosines of light ray against the x and y axes, respectively. When satisfying a paraxial approximation condition, i.e., $[(u-x)^2+(v-y)^2+f^2]^{1/2} \approx f$ (f denotes the axial displacement between the two planes), it can derive from Eq. (1) that

$$\frac{\partial \Psi_1}{\partial x} = ka_1 \approx k\frac{u-x}{f}, \qquad \frac{\partial \Psi_2}{\partial y} = kb_1 \approx k\frac{v-y}{f}. \tag{2}$$

Mathematically, if the second-order partial differentiations of Ψ_1 exists and are continuous, the order of differentiation is immaterial. Hence, a sufficient but not necessary condition to be concluded is $\partial u/\partial y = \partial v/\partial x$.[34,35] To correct the parallel output of light rays, the direction cosines on the phase plane Ψ_2 follow $a_2 = -a_1$ and $b_2 = -b_1$, and the phase gradient satisfies

$$\frac{\partial \Psi_2}{\partial x} = ka_2 \approx -k\frac{u-x}{f}, \qquad \frac{\partial \Psi_2}{\partial y} = kb_2 \approx -k\frac{v-y}{f}. \tag{3}$$

Building upon this, we have considered the mode multiplication of CVB by controlling the light rays distributed from the whole annulus to an annular sector, as depicted in Fig. 1. Here we stipulate that $\Psi_1(r, \varphi)$ serves as the first phase plane for implementing the light ray modulation while $\Psi_2(\rho, \theta)$ is correction phase plane for collimating the output beam, both in polar coordinates [Fig. 1(a)]. Utilizing rescaling operation in azimuthal coordinate to specify the trajectory of light rays, it is $\theta = \varphi/N$ (N is the positive or negative integer multiplier factor demanding $|N| > 1$), and the radial coordinate mapping can be solved as $\rho = \alpha(r/\beta)^{-1/N}$ according to the condition of $\partial u/\partial y = \partial v/\partial x$. To reconstruct the entire multiplicated CVB structure, it is imperative to undergo multifold annulus-sector transformations, as showcased in Fig. 1(b). Specifically, the input CVB mode are mapped into multiple adjacent complementary sectors with identical angle ranges of $2\pi/|N|$ and centered on $2\pi(i-1)/N$, $i = 1, 2, \ldots, |N|$. Thus, the azimuthal coordinate mapping for each sector can be expressed as $\theta_i = (\varphi/N) + [2\pi(i-1)/N]$. Substituting the above coordinate mapping expressions to the partially differential equations (2) and (3), together with the conversion between polar and Cartesian frames, the phase functions for the first and second planes can be calculated by

$$\Psi_1 = \text{angle}\Big\{ \sum_{i=1}^{|N|} \exp\Big[j \cdot \frac{k\alpha\beta(r/\beta)^{1-1/N}}{f} \cdot \frac{\cos(\varphi - \varphi/N - 2\pi(i-1)/N)}{1-1/N} - \frac{jkr^2}{2f} \Big] \Big\}, \tag{4}$$

$$\Psi_2 = \text{angle}\Big\{ \exp\Big[j \cdot \frac{k\alpha\beta(\rho/\alpha)^{1-N}}{f} \cdot \frac{\cos(N\theta - \theta)}{1-N} - \frac{jk\rho^2}{2f} \Big] \Big\}. \tag{5}$$

Here α and β are constant scaling parameters that can tune the coordinates ρ, r separately and control the ring size of output annulus jointly; j represents an imaginary unit; f is the diffraction distance between two planes and determines the focus degree of light field on the image plane. As a result, with the flexibly defined multiplier factor N and solved phase modulation functions (Ψ_1, Ψ_2), this approach enables multiple CVB modes carrying different polarization orders (such as $m = -2$, -1, $+1$, $+2$) to be performed with an N-fold mode multiplication conversion, thereby obtaining the scaled-up output polarization orders of $m = -2N$, $-1N$, $+1N$, $+2N$, respectively, as illustrated in Fig. 1(c).

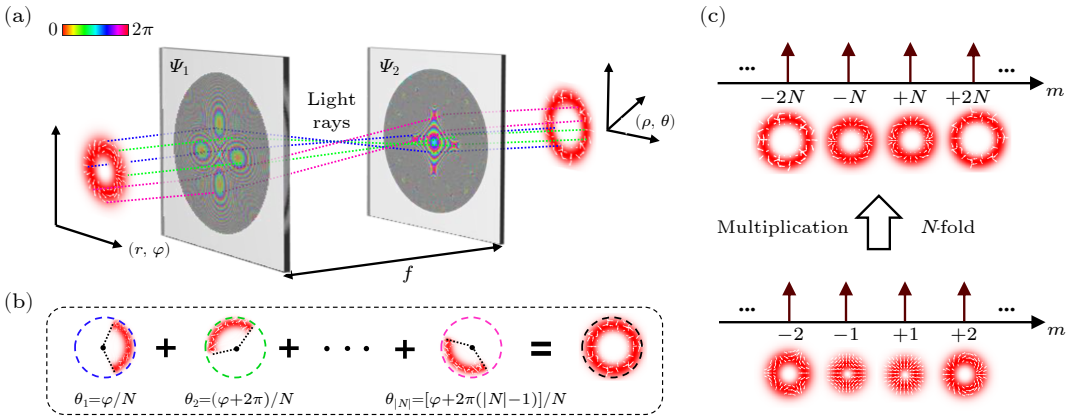

Fig. 1. Principle of CVB mode multiplication. (a) Schematic of raytracing procedure for multiplying a CVB mode between two phase planes. (b) Description of multifold annulus-sector transformations. (c) Theoretical expectation of a N-fold CVB mode multiplication conversion via the proposed scheme.

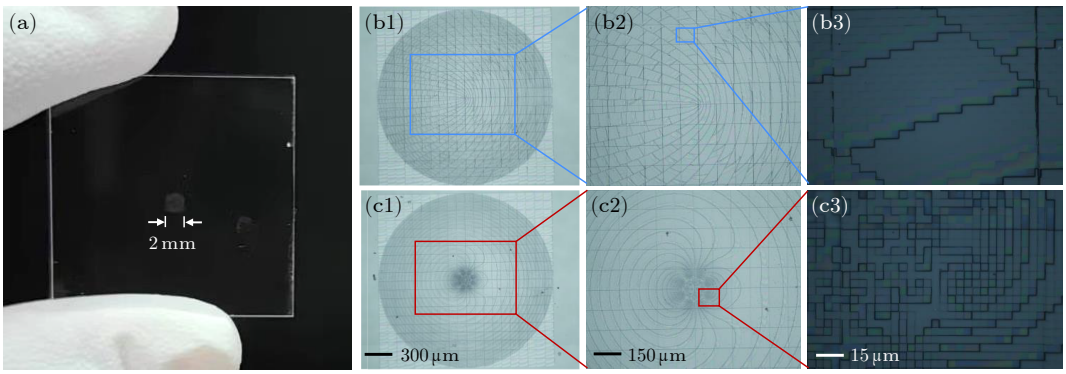

Fig. 2. Characterization of the fabricated +2-fold mode multiplier. (a) Captured photograph of the sample. (b1)–(b3) Microscopic images of the device used for the first phase plane Ψ_1. (c1)–(c3) Microscopic images of the device used for the second phase plane Ψ_2.

The raytracing control strategy for CVB manipulation requires the local polarization features of vector mode to be preserved along with multiplication operation, behaving as a phase-only modulation for the inhomogeneous vector wavefront. Consequently, we designed and fabricated the polarization-insensitive CVB mode multipliers to response the phase modulation functions (Ψ_1, Ψ_2) by employing a two-photon nanolithography (TPN) technique.[36,37] Without loss of generality, we explored the proof-of-concept demonstrations for CVB mode multiplication within the multiplier factors of $N = +2$ and $N = -3$, respectively. After meticulously determining the parameters ($\alpha = 300\,\mu$m, $\beta = 300\,\mu$m, $f = 20\,$mm, $\lambda = 1550\,$nm) and properly solving the phase modulation functions (Ψ_1, Ψ_2), two pairs of CVB mode multipliers were obtained by fabricating. The elaborate description of fabrication process is provided in Note S1 of the Supplementary Material. Figure 2 presents the characterization of the fabricated +2-fold mode multiplier, while for the −3-fold mode multiplier is included in Supplementary Material Note S2. Figure 2(a) shows an actual photograph of the fabricated device used for the first phase plane Ψ_1, which is positioned on a 0.7-mm-thick square SiO_2 substrate with a footprint of $2.5 \times 2.5\,$cm^2. In the middle 2-mm-diameter working area is the cured photoresist (IP-Dip) induced by the femtosecond laser with a power of 22 mW. To facilitate fabrication, we have structured the desired phase profile in an array format of 500×500, with a square unit size of 4 μm. The surface morphology of the fabricated multiplier was captured by using a metallurgical microscopy (ECLIPSE LV150N), as shown in Fig. 2(b) for the first phase plane Ψ_1 and in Fig. 2(c) for the second counterpart Ψ_2. The 2 mm square region is made up of medium squares with pixels of 20×20, in which insert 25×25 square fabrication units. By stepping lithography in larger squares, it is convenient to prepare the designed phases. With a careful two-plane alignment cascade, the desired CVB mode multiplication is permitted. Remarkably, these square pixel structures guarantee that the obtained device is polarization-insensitive, which is essential for the phase-only modulation required for operating CVB mode multiplication.

To verify the proposed strategy's feasibility in multiplying CVB modes, we constructed a dedicated measurement apparatus combined with the fabricated multiplier devices, and these details are outlined in Supplementary Material Note S3. Figure 3(a) portrays the chosen input CVB modes (with the polarization order m of −2, −1, +1,

+2, respectively), created by converting the fundamental Gaussian modes into the non-uniform vector modes utilizing the combination of a Q-plate (with the q-values of 1 or 0.5) and a half-wave plate. The polarization order of the CVB mode allows to be directly detected by employing a linear polarizer (LP) with varying transmission directions, as seen in Fig. 3. Specifically, the number of the generated side lobes signifies twice polarization order of the CVB mode, and its sign is positive when the side lobes rotate in the same direction as the transmission axis of the LP and vice versa. Achieving mode multiplication with the designed multipliers ($N = +2$ and $N = -3$), the intensity and polarization distributions of output CVB modes were measured as indicated in Figs. 3(b) and 3(c). From the polarization detection results, these four input CVB modes were successfully implemented the multiplicative conversions, which are in good agreement with the theoretical expectations. The white arrows drawn on the output intensities represent the measured polarization patterns on the CVB cross section, which were numerically calculated using the method of Stokes polarimetry (see Supplementary Material Note S4). Notably, the results of −3-fold CVB mode multiplication exhibit the darker intensities. This reason comes from the fact that operation with a larger multiplier factor $|N|$ require more superimposed phases [see Eq. (4)], which results in a reduced diffraction efficiency due to the multi-level transformations. Nevertheless, the measured diffraction efficiencies in our experiments are still higher than 90.38% and 84.31% for $N = +2$ and $N = -3$, respectively (see Supplementary Material Note S5). Despite errors due to fabrication and misalignment, the achieved results confirm the validity of our approach for CVB mode multiplication.

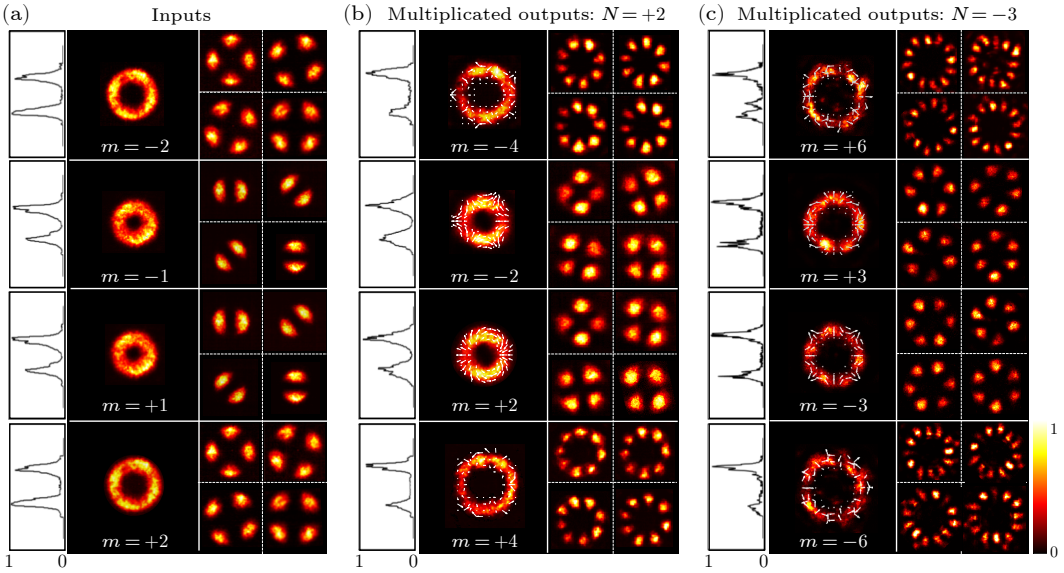

Fig. 3. Experimental results of CVB mode multiplication. (a) Captured intensities and polarization detection results of four selected input CVB modes. Measured intensities, polarization patterns, and polarization detection results of multiplicated output CVB modes in the multiplier factors of (b) $N = +2$ and (c) $N = -3$. The left column shows the intensity curves of CVBs along the center-vertical direction, and the polarization detection depends on the transmission direction of LP, i.e., 0°, 45°, 90°, and 135°.

We further measured the purities of multiplicated output CVB modes for $N = +2$ and $N = -3$, as presented in Figs. 4(a) and 4(b). The mode purity was obtained by degrading the output CVB mode to a fundamental Gaussian mode through a proper Q-plate and calculating the power ratio of the Gaussian spot to the total output intensity. As is seen, the converted mode purities exceed 94.24% and 88.37% in the multiplier factors of $N = +2$ and $N = -3$, respectively. In addition to supporting a single mode input, the proposed multiplier is also capable of performing multi-mode parallel multiplicative operation. To further demonstrate this, we constructed a two-channel CVB mode multiplication link (see the optical setup in Supplementary Material Note S6). Figures 4(c) and 4(d) depict the measured input-output intensity distributions of CVBs before and after mode multiplication, which is consistent with the theoretical expectations. Due to the independence of mode multiplication, the proposed multiplier can also be extended to other input modes (see Supplementary Material Note S7).

To reveal the potential application of the designed mode multiplier in channel switching within CVB multiplexing communication, we constructed a four-channel CVB multiplexing communication system with simultaneous PDM (see Supplementary Material Note S6), including two CVB modes and two polarizations. The multiplier is polarization-insensitive, which enables it to be compatible with radial and azimuthal CVB modes, thus allowing for PDM. Specifically, 200 Gbit/s QPSK signals carried by these four channels were successfully switched upon CVB

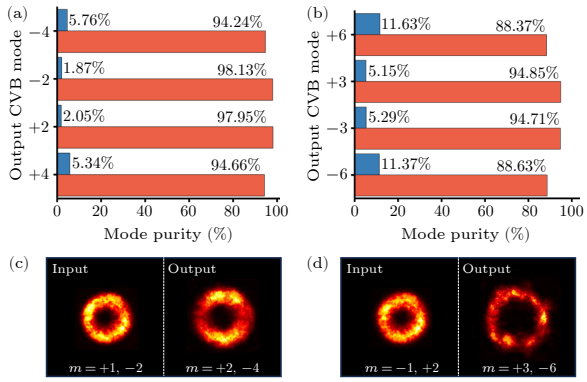

Fig. 4. Measured results of mode purity and a two-channel CVB mode multiplication. Mode purities of multiplicated output CVB modes in the multiplier factors of (a) $N = +2$ and (b) $N = -3$. Input-output intensity distributions within multiplication of two CVB modes for (c) $N = +2$ and (d) $N = -3$.

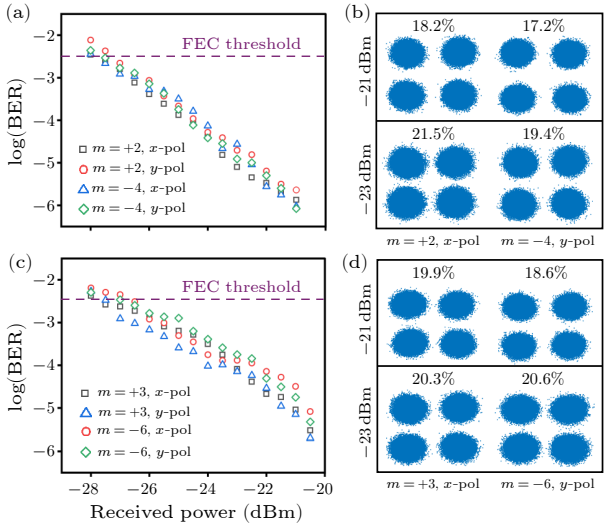

Fig. 5. Communication results of channel switching based on CVB mode multiplication. (a) BER curves and (b) partial constellation diagrams of mode signals upon the +2-fold CVB mode multiplication. (c) BER curves and (d) partial constellation diagrams for the −3-fold mode multiplication. "FEC threshold" denotes the hard-decision forward error correction threshold of 3.8×10^{-3}. "$m = +3$, x-pol" represents the output CVB channel with the polarization order of +3 in an x-polarization input, and the others are expressed similarly.

mode multiplication conversion. With the +2-fold and −3-fold mode multipliers, the measured BER curves of the four channels versus different received optical powers are plotted in Figs. 5(a) and 5(c), respectively. All BERs approach 1×10^{-6} as the received optical power increases to −20 dBm. Furthermore, their partial constellation diagrams and corresponding error vector magnitudes (EVMs) at the received optical power of −21 dBm and −23 dBm are presented in Figs. 5(b) and 5(d), respectively. The measured constellations are highly convergent, and the EVMs are lower than 21.5%. These findings suggest that the proposed mode multipliers are effective and reliable for channel switching in CVB multiplexing communication.

In this study, we are dedicated to achieving the multiplicative operation in CVB modes by utilizing a raytracing control strategy. This scheme imparts the multifold conformal annulus-sector mappings into a pair of polarization-insensitive phase modulations, facilitating CVB mode multiplication with conserved vector structure. With the fabricated mode multipliers via the TPN method, we have successfully demonstrated the multiplication of four CVB modes with the multiplier factors of $N = +2$ and $N = -3$, obtaining the converted mode purities up to 94.24% and 88.37%, respectively. Building upon this foundation, 200 Gbit/s QPSK signals were successfully transmitted and switched with the BER approaching 1×10^{-6}. Our demonstration represents a significant advancement in CVB mode conversion by developing a previously unreported CVB mode multiplication technique, breaking the fixed constraint over mode shift operation. Although only two-mode multiplication was demonstrated in our validation, the proposed route is universal, as further affirmed by altering the multiplier factor N and adjusting the corresponding parameters of α, β, and f (see Supplementary Material Note S8). Owing to the sector composition of our method, the universality can be extended to light beam modes endowed with angular periodicity, which is common in circular symmetric structure light beams. A set of linear polarized (LP) modes like LP_{11}, LP_{21}, LP_{31} that transmitted in optical fiber also satisfy the symmetry, but it is quite difficult for elaborate mode control in free space to meet the transmission restriction of fibers. Moreover, in the time reversal direction, the proposed mode multiplier permits the division of CVB modes during the targeted mode in the reverse incidence, but it comes at the cost of a power loss of about $(|N| - 1)/|N|$. It is important to note that this strategy can also be extended to other fields related to conformal mapping, such as the recent multi-ring transform and spiral transform.[26,28,38] We believe that this scheme can promote the development of mode operation and its advanced applications towards CVB multiplexing communication.

Acknowledgments. This work was supported by the National Natural Science Foundation of China (Grant No. 62271322), the Guangdong Basic and Applied Basic Research Foundation (Grant No. 2023A1515030152), the Shenzhen Science and Technology Program (Grant No. JCYJ20210324095610027), and the Natural Science Foundation of Top Talent of SZTU (Grant No. GDRC202204). The authors also acknowledge the technical assistance from Photonics Research Centre of Shenzhen University.

References

[1] Yu Y, Xu M, Pu M, Ding J, Chen S, Zhang Y, Zhou M, Guo Y, Li X, Ma X, and Luo X 2023 *Opt. Express* **31** 42165

[2] Zhang Y H, Liu S J, Chen P, Zhu D, Chen W, Ge S J, Wang Y, Zhang Z F, and Lu Y Q 2024 *Nat. Commun.* **15** 1108

[3] Shen Y, Zhang Q, Shi P, Du L, Yuan X, and Zayats A V 2024 *Nat. Photon.* **18** 15
[4] He C, Shen Y, and Forbes A 2022 *Light Sci. Appl.* **11** 205
[5] Wan Z, Wang H, Liu Q, Fu X, and Shen Y 2023 *ACS Photon.* **10** 2149
[6] He Y, Wang X, Yang B, Cheng M, Xie Z, Wang P, Ye H, Liu J, Li Y, Yang Y, Fan D, and Chen S 2022 *J. Light. Technol.* **40** 5070
[7] Chen S, Xie Z, Ye H, Wang X, Guo Z, He Y, Li Y, Yuan X, and Fan D 2021 *Light Sci. Appl.* **10** 222
[8] Jia Q, Zhang Y X, Shi B J, Li H, Li X X, Feng R, Sun F K, Cao Y Y, Wang J, Qiu C W, and Ding W Q 2023 *Nanophotonics* **12** 3955
[9] Zhou C, Liang W, Xie Z, Ma J, Yang H, Yang X, Hu Y, Duan H, and Yuan X 2024 *Nat. Commun.* **15** 4022
[10] He Y, Huang Z, Li C, Yang B, Xie Z, Wu H, Wang P, Li Y, Yang Y, Fan D, and Chen S 2022 *Opt. Lett.* **47** 6341
[11] Ahmed N, Huang H, Ren Y, Yan Y, Xie G, Tur M, and Willner A E 2014 *Opt. Express* **22** 756
[12] Liu J and Wang J 2016 *Sci. Rep.* **6** 37331
[13] Lei T, Gao S, Li Z, Yuan Y, Li Y, Zhang M, Liu G N, Xu X, Tian J, and Yuan X 2017 *IEEE Photon. J.* **9** 7901409
[14] Hua Y L, Wang Z Q, Li H L, Gao N, and Du Y C 2012 *Chin. Phys. Lett.* **29** 084214
[15] Nazemosadat E, Mazur M, Kruk S, Kravchenko I, Carpenter J, Schröder J, Andrekson P A, Karlsson M, and Kivshar Y 2019 *Adv. Opt. Mater.* **7** 1801679
[16] Fang B, Wang Z, Li Y, Ji J, Xi K, Cheng Q, Shu F, Jin Z, Hong Z, Zhan C, Shen C, and Li T 2023 *Photon. Res.* **11** 2194
[17] Guo Y H, Zhang S C, Pu M B, He Q, Jin J J, Xu M F, Zhang Y X, Gao P, and Luo X G 2021 *Light Sci. Appl.* **10** 63
[18] Qiu Y, Tang S, Cai T, Xu H, and Ding F 2021 *Front. Optoelectron.* **14** 134
[19] Kostyuk G, Shkuratova V, Petrov A, Stepanyuk D, and Zakoldaev R 2023 *Opt. Quantum Electron.* **55** 344
[20] Liu X, Zhou J, Xue J, and Meng Z 2022 *Laser Phys.* **32** 035402
[21] Brandt F, Hiekkamäki M, Bouchard F, Huber M, and Fickler R 2020 *Optica* **7** 98
[22] Shen D, He T, Yu X, and Zhao D 2022 *IEEE Photon. J.* **14** 1
[23] Ayoub A B and Psaltis D 2021 *Sci. Rep.* **11** 18837
[24] Ruffato G and Kobayashi H 2021 *Opt. Commun.* **490** 126893
[25] Cheng J, Wan C, and Zhan Q 2023 *Opt. Lett.* **48** 1762
[26] Yao Q, Cheng J, Liu W, and Wan C 2024 *Opt. Lett.* **49** 81
[27] Wang B, Wu L, Lin Z, Zhong W, Zhu Z, and Chen Y 2024 *Laser Photon. Rev.* 2400113
[28] Zeng Z, Pang Z, Pan K, Xu J, and Zhao D 2023 *Photon. Res.* **11** 165
[29] Ruffato G, Massari M, and Romanato F 2019 *Light Sci. Appl.* **8** 113
[30] Cao H, Liang Y, Wang L, Ruan Z, Wang H, Zeng J, and Wang J 2023 *Laser Photon. Rev.* **17** 2200631
[31] Yao Q, Liu W, Cheng J, Liang Q, and Wan C 2024 *ACS Photon.* **11** 2459
[32] Zheng S, Li Y, Lin Q, Zeng X, Zheng G, Cai Y, Chen Z, Xu S, and Fan D 2018 *Photon. Res.* **6** 385
[33] Lin Z, Xie Z, He Y, Wang X, Wu H, Wang S, Guan Z, Liu J, Ye H, Li Y, Fan D, and Chen S 2021 *Opt. Lett.* **46** 5563
[34] Bryngdahl O 1974 *J. Opt. Soc. Am.* **64** 1092
[35] Hossack W J, Darling A M, and Dahdouh A 1987 *J. Mod. Opt.* **34** 1235
[36] Wang H, Zhang W, Ladika D, Yu H Y, Gailevičius D, Wang H T, Pan C F, Nair P N S, Ke Y J, Mori T, Chan J Y E, Ruan Q F, Farsari M, Malinauskas M, Juodkazis S, Gu M, and Yang J K W 2023 *Adv. Funct. Mater.* **33** 2214211
[37] Goi E, Schoenhardt S, and Gu M 2022 *Nat. Commun.* **13** 7531
[38] Cheng J and Wan C 2023 *Opt. Lett.* **48** 6124